12th AIAA Aviation Technology, Integration, and Operations (ATIO) Conference and 14th AIAA/ISSM
17 - 19 September 2012, Indianapolis, Indiana

AIAA 2012-5474

Performance Analysis and Design of On-Demand Electric Aircraft Concepts

Michael D. Patterson* and Brian J. German†
Georgia Institute of Technology, Atlanta, GA, 30332, U.S.A.
Mark D. Moore‡
NASA Langley Research Center, Hampton, VA, 23681, U.S.A.

The work presented in this paper is part of a larger NASA study focused on investigating the characteristics and feasibility of an on-demand air transportation system that consists of a fleet of small, electrically-powered, general aviation aircraft. The present paper focuses on the performance and design implications of using electric propulsion systems for these on-demand aircraft. As a part of this study, a procedure to create aircraft performance models has been developed. The procedure is used to model a Cirrus SR-22 aircraft to serve as a point of comparison and to establish confidence in the approach for application to electric concepts. Simple performance and sizing tools are developed for battery electric concepts, and calculations are performed using these tools to study the feasibility of fully electric aircraft for on-demand missions. Results indicate that designing electric aircraft through simple modifications of existing airframes are not likely to produce aircraft with practical range capability in the near term; however, innovative vehicle concepts designed to leverage specific opportunities available with battery-electric propulsion show promise in meeting performance targets as soon as 2015.

Nomenclature

A	Area	SFC	Specific fuel consumption
C_D	Drag coefficient	T	Thrust
C_{D0}	Parasite drag coefficient	t	Time
C_f	Skin friction coefficient	u	Energy Density
C_L	Lift coefficient	V	Velocity
D	Drag	W	Weight
E	Energy	η	Efficiency
FF	Form factor	κ	Fraction
g	Acceleration due to gravity	Λ	Exhaust angle
L	Lift	ρ	Density
m	Mass		
N	Endurance	Subscripts	
P	Power	avail	Available
p	Pressure	bat	Batteries
Q	Interference Factor	elec	Electrical system
R	Range	prop	Propeller
ROC	Rate of climb	req	Required
S	Wing area	t	Total
s	Distance	∞	Freestream

*Graduate Research Assistant, School of Aerospace Engineering, 270 Ferst Drive. Student Member AIAA.
†Assistant Professor, School of Aerospace Engineering, 270 Ferst Drive. Senior Member AIAA.
‡Aerospace Engineer, Aeronautics Systems Analysis Branch, NASA Langley, MS 442, AIAA Member.

I. Introduction & Motivation

In 2011, the NASA/CAFE Foundation Green Flight Challenge sought to "push technology and make passenger aircraft more efficient."[1] Specifically the competition was targeting full aircraft systems that could achieve over 200 passenger-miles per gallon while flying at least 100 mph for 200 miles. Entries to the competition included aircraft powered by bio fuels, hybrid electric propulsion systems, and fully electric designs. The top two prizes in the competition were taken by fully electric aircraft, which each demonstrated over 375 passenger-miles per gallon equivalent. While dismissed by some as impractical "novelties," the Green Flight Challenge helped showcase that electric aircraft are becoming more practical and can achieve incredibly efficient flight; in fact NASA's chief technologist Joe Parrish remarked at the Green Flight Challenge, "Today we've shown that electric aircraft have moved beyond science fiction and are now in the realm of practice."[2]

Electric aircraft are receiving increased attention not just for their potential in eliminating emissions, but also for the substantial reductions in noise and increases in efficiency and reliability that can be achieved. Due to low vibration levels and substantially fewer parts than conventional internal combustion engines, electric motors require less maintenance than traditional engines, which may improve reliability and reduce operational cost. The low cost of electricity when compared to conventional fuels also helps reduce operating costs. Electric propulsion systems are also synergistic with many renewable energy technologies, such as solar photovoltaic cells, and with more electric aircraft initiatives, where hydraulics and other aircraft subsystems are being replaced by electrically-driven components. Electric motors require smaller volumes and weigh less than traditional internal combustion engines, which may allow for increased payload capacity, reduced wetted area, and the ability to use redundant motors with minimal penalties. In addition to potential power redundancy, the ability to provide an emergency power supplement for 30 seconds or more through motor heat saturation can further improve aircraft safety.

There will be differences in the benefits attainable by retrofitting existing aircraft with fully-electric propulsion systems and designing completely new aircraft around electric propulsion. Aircraft that implement battery-electric propulsion systems have radically different characteristics, such as no power lapse with altitude and no weight loss through fuel burn, that violate conventional design assumptions for reciprocating and turbine engines. Additionally, there are increased integration benefits possible between the propulsion system and airframe such as the ability to distribute thrust in many locations with small lightweight motors that may fundamentally alter the way aircraft are designed and operated. These vehicles may also be able to replenish some of their energy supply in mid-flight without requiring another aircraft by utilizing solar photovoltaic cells, wingtip vortex turbines,[3,4] or other technologies, which may influence the required aircraft size.

Electric aircraft are not without disadvantages, however. There are many regulatory issues involved in the practical adoption of fully electric aircraft into the air transportation system including certification standards that are currently written specifically for aircraft with traditional internal combustion engines. In addition to regulatory issues, there are also technical challenges associated with fully electric aircraft. The issue of storage capacity represents a major hurdle in the widespread, practical use of fully electric aircraft. The energy density of battery technologies is currently one to two orders of magnitude lower than that of conventional fossil fuels. While the weight of electric motors is considerably less than that of internal combustion engines and the efficiency of electric motors is considerably higher, the low energy density of the "fuel"—electricity stored in batteries—currently leads to much higher total air vehicle weights for the same amount of practical energy. The quantification of the gap between electrically-driven aircraft and fossil fuel-driven aircraft requires the development of accurate models of both types of propulsion systems and the aircraft on which they are employed.

While propulsion systems can be analyzed independently of any other aircraft subsystems or the system as a whole, full aircraft system studies are needed to assess the true potential of fully electric propulsion. Studying electric propulsion systems with current vehicle designs in mind may lead to incorrect assumptions or inappropriate limits on what electric propulsion systems may be able to accomplish. The design and operation of fully electric aircraft will likely be impacted by such a fundamentally different propulsion system. Studies that appropriately indicate integrated vehicle-level benefits are only possible if the propulsion system is considered as a part of the entire aircraft system.

A. On-demand Aircraft Concept

The studies in this paper are centered on small, general aviation aircraft for use in an on-demand air transportation system. This effort is part of a broader NASA initiative, which seeks to model not only the performance of individual aircraft, but also an entire system of systems concept for on-demand transportation including the operating model, economics, and emissions. The system operational concept is called 'Zip Aviation' and is derived from a current trend towards achieving lower cost of ownership for automobiles through car-sharing. Several additional works address other aspects of this transportation model, including a demand and airspace impact study;[5] a concept of operations;[6] the degree, cost, and safety of aircraft automation; and more aggressive advanced concepts that attempt to take advantage of the unique characteristics that electric propulsion offers.[7,8] This additional work lays the foundation for a fleet of highly autonomous, electric aircraft that can operate from 10,000 airfields currently available across the U.S. that have at least 2,000 foot field lengths. The objective is to showcase the potential for very low operating costs, over relatively short 200 mile ranges, and achieve very high utilizations of 1,500 hours per year through high reliability and a large user base resulting from the ease of use of the proposed vehicles. This paper describes initial work to understand the performance and design considerations for the small, electrically-powered, general aviation class aircraft intended to operate in this on-demand transportation role. The present study seeks to determine the required size and design characteristics of these on-demand concepts, while exploring the differences between traditional aircraft design assumptions and the design issues associated with fully electric aircraft.

This paper begins by describing the modeling procedure used to estimate vehicle performance. The procedure is then implemented to model the performance of the Cirrus SR-22 single-engine, piston, general aviation aircraft to calibrate and validate the modeling approach and to produce baseline results for comparison to the envisioned electric aircraft concepts. Simple Breguet-like range analysis methods for estimating the mission performance of electric aircraft are developed and used to study the impacts of retrofitting an SR-22 airframe with an electric propulsion system using various technology assumptions. A method of sizing battery-electric aircraft is then developed and the required weight, wing size, and power of these aircraft are computed for several sets of technological assumptions corresponding to anticipated entry-into-service years. The impacts of various system-level parameters on the required aircraft size are studied and several design rules for small, general aviation class, fully electric aircraft are proposed.

II. Modeling Procedure and Baseline Model Calibration

The ability to develop baseline models that accurately reflect the performance of existing aircraft is essential to establish a meaningful comparison to new battery-electric aircraft concepts. These comparisons can help illustrate the differences—both beneficial and detrimental—between these conventional and fully electric concepts. Modeling must be performed at a level of detail that will fairly and adequately capture the differences between the concepts under consideration. Specifically in the comparison of electrically- and conventionally-powered aircraft, accurate, generic models must be developed that apply to both propulsion systems types and are able to capture the fundamental differences between the use of these different propulsion systems.

In addition to providing a point of comparison for performance, the development of baseline models can help refine and validate a modeling process. If, in baseline model creation, deficiencies in a modeling process are observed, these can be remedied before studying advanced concepts. Confidence in the accuracy of the modeling procedure can be established if accurate performance models for one or multiple baseline aircraft are created using the procedure.

This section describes the modeling process that was used to develop performance models of a Cirrus SR-22 general aviation (GA) aircraft for the purpose of comparing this aircraft to new electric aircraft concepts and validating the modeling procedure. The final performance models are developed in NASA's Flight Optimization System (FLOPS)—an aircraft analysis and optimization tool that has been widely used for modeling aircraft performance.[9,10] The Cirrus SR-22 is a common, 4 passenger, single-engine, piston/propeller aircraft that has been used extensively by several "air taxi" on-demand carriers including ImagineAir,[11] Skyway Air Taxi,[12] OpenAir,[13] and SATSair. The SR-22 is state-of-the-art in terms of available general aviation technologies. Additionally, reliable and detailed information sources such as a pilot's operating handbook (POH)[14] are available to ensure that the models developed are well-calibrated and accurately model the aircraft performance across the flight envelope.

A. Geometry Modeling

In our modeling procedure, the vehicle geometry is described using NASA's OpenVSP (Vehicle Sketch Pad).[15,16] OpenVSP (VSP) is an excellent tool for quickly defining the vehicle geometry and determining all the geometric parameters required for a FLOPS performance model, including parameters that are difficult to approximate based only on a POH or 3-view drawing. VSP provides wetted area and volume information, which can be useful for aerodynamic modeling and studying internal layout of the vehicle. Other information that is needed for the aerodynamic modeling such as average thickness to chord ratios, fineness ratios, and average chord lengths can be quickly exported directly from VSP.

A VSP model of the SR-22 was created to begin the modeling process. A rendering of this model is shown in Fig. 1. The airfoil used on the SR-22 wing is of a proprietary design. Due to the lack of information, a

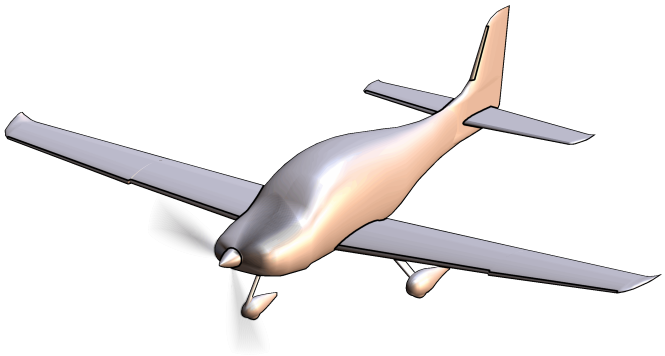

Figure 1. SR-22 VSP Geometry Model

laminar flow airfoil used on an older Cirrus aircraft, the NASA NLF(1)-0414F, was modeled. This airfoil was thought to embody some of Cirrus's design philosophies and exhibited properties of the actual airfoil such as large portions of laminar flow. Information about the tail airfoils was also unavailable; therefore, a symmetric NACA 4-series airfoil was selected.

B. Aerodynamics

Aerodynamic models including all forms of drag—skin friction, form, profile, wave, interference, cooling, and induced—can be produced after the geometry of the aircraft is fully defined. The methods employed in the modeling procedure account for differences in propulsion systems and help quantify with more detail components of drag that are typically crudely estimated. The intent of the detailed aerodynamic modeling approach is to capture as many differences between traditional aircraft and new fully electric on-demand concepts as possible. For the SR-22 modeling, all of the drag calculations were performed at an altitude of 8,000 ft and a speed of 180 knots—a reference cruise condition quoted in SR-22 promotional materials,[17] which was assumed to be a design point used by the manufacturer.

For the modeling in the current study, the induced drag estimations are made with XFLR5, an open source vortex lattice tool.[18] This program also estimates the profile drag due to lift and the turbulent boundary layer transition location for the lifting surfaces of the aircraft based on an extrapolation of 2-D airfoil analyses.

In the SR-22 modeling, only the main lifting surfaces—the wing and the horizontal tail—were included in the XFLR5 model. Because almost no information was known about the twist distribution of the wing, the twist distribution was adjusted so that the resulting total lift distribution (including the wing and tail) was as close to elliptic as possible by using only simple linear variations in twist. The resulting maximum span efficiency was found to be 0.948. Also, the incidence angle of the horizontal tail was set such that the aircraft would trim at the reference flight condition.

In order to estimate the skin friction, form, and interference drag, a component drag buildup method was used.[19] This model uses flat plate skin friction coefficients modified by form factors and interference factors to estimate the drag on each component (i.e., wing, fuselage, etc.) of the aircraft. The form factors were calculated using the regressions developed by Feagin and Morrison that are also used in the internal

aerodynamic estimations of FLOPS.[20] The interference factors and the percentage of laminar flow over non-lifting components necessary for a component drag buildup were estimated using engineering judgment and guidelines from the literature,[19] and the percentage of laminar flow over lifting surfaces was approximated using XFLR5 results.

The drag from the interaction of the propeller slipstream with the airframe was also considered. This "scrubbing drag" was estimated by determining the increased velocity of the flow behind the propeller and then using this velocity instead of the freestream velocity in the drag buildup method for only the component(s) over which the slipstream flows. A simplified actuator disk model that assumes steady, inviscid, incompressible flow is used to determine the velocity behind the propeller. The propeller disk area (A), the blockage area behind the propeller (A_{blockage}), the freestream velocity (V_∞), freestream density (ρ_∞), engine/motor shaft power (P), and the propeller efficiency (η_{prop}) can be used to estimate the velocity of the slipstream behind the propeller using Eq. 1.

$$V_{\text{slipstream}} = \frac{V_\infty}{2} + \sqrt{\left(\frac{V_\infty}{2}\right)^2 + \frac{P\eta_{\text{prop}}}{2\left(A - A_{\text{blockage}}\right)\rho_\infty V_\infty}} \tag{1}$$

The slipstream velocity, $V_{\text{slipstream}}$, is used to calculate the Reynolds number for components with propeller scrubbing in the component drag buildup number. After determining the skin friction coefficient of the component with propeller scrubbing (C_f), the parasite drag coefficient of the component in the propeller slipstream can be calculated as follows:

$$C_{D0,\text{c}} = \frac{\left(C_{f,\text{c}}\right)\left(FF_\text{c}\right)\left(Q_\text{c}\right)\left(S_{\text{wet,c}}\right)}{S}\left(\frac{V^2_{\text{slipstream}}}{V^2_\infty}\right) \tag{2}$$

where the subscript c denotes that it is for a specific component. The velocity fraction $V^2_{\text{slipstream}}/V^2_\infty$ is necessary to convert the drag coefficient calculated with reference to the slipstream velocity to the drag coefficient relative to the reference flight condition. For the SR-22, scrubbing drag was considered only on the fuselage, and this drag was calculated assuming a propeller efficiency of 0.81, an engine power setting of 75%, and a blockage area of 3.64ft^2, which was estimated from the VSP model.

The drag from propulsion system cooling airflow, known as "cooling drag," is an often-neglected form of drag that will likely differ considerably between traditional internal combustion engines and electric motors. Cooling drag results from the momentum loss of airflow that must be passed over the engine or electric motor in order to cool the device and any pressure differential between the exit and inlet. This drag can be estimated for traditional aircraft using "rule of thumb" estimations from Corsiglia et al.[21] or Katz et al.;[22] however, these semi-empirical methods have been calibrated only for internal combustion engines. In order to assess the drag from both internal combustion engines and electric motors, a novel cooling drag estimation approach was developed. The approach models the cooling system as a generic propulsion system similar to a ramjet and determines the "thrust" of that system. Ram drag will typically dominate gross thrust associated with flow heating resulting in negative net thrust, or, positive cooling drag. The cooling drag can be found from Eq. 3 where the $\cos\left(\Lambda\right)$ term represents the effects of exhausting the cooling airflow at an angle of Λ to the freestream.

$$D_{cool} = \dot{m}_{cool}\left(V_\infty - V_{exit}\cos\left(\Lambda\right)\right) + \left(p_\infty - p_{exit}\right)A_{exit}\cos\left(\Lambda\right) \tag{3}$$

This cooling drag model requires information about the operating temperatures of the engine or motor and the total pressure loss through the cooling system to determine all the parameters required in Eq. 3. Specifically, the required cooling airflow rate is determined by the amount of "waste heat," which is a function of engine or motor operating temperature. The mass flow rate of cooling airflow is set by the exit area of the cooling system, which can be either fixed or variable with the use of cowl flaps. For aircraft with a fixed cooling system exit area, the exit area must be sized to a critical cooling "on-design" condition; this fixed exit area will cause greater cooling drag at "off-design" conditions. The model developed is capable of handling both on-design and off-design analyses and can be used to estimate the cooling drag for aircraft with and without cowl flaps.

To account for the variation of cooling drag with flight condition, the corrected drag—a parameter analogous to corrected thrust, which is sometimes used in propulsion system design[23]—is employed. The corrected drag is defined as $D_{corrected} \equiv D/\delta_0$, where $\delta_0 = p_{t,\infty}/p_{\text{SL}}$, $p_{t,\infty}$ is the freestream total pressure, and

p_{SL} is sea level static pressure. The corrected drag is employed because it was found to exhibit substantially less variation with operating condition than dimensional drag. For the cooling drag model, the corrected drag was treated as constant across varying operating conditions. The constant corrected drag was input directly into a modified version of FLOPS used for the study presented in this paper.

The cooling drag of the SR-22 was estimated with this model. Because the SR-22 does not have cowl flaps, a critical cooling point was selected to size the cooling system—a climb on a hot day at sea level. The hot day was defined as a 41°F above standard temperature,[24] and climb power settings based on information in the POH were selected. The resulting off-design analysis holding the exit area constant at the reference cruise conditions indicated a cooling drag of 16.75 lb; this dimensional drag corresponds to a corrected cooling drag of 21.4 lb and approximately 6% of the total aircraft drag at the reference conditions, which is in line with the rule of thumb estimations.[21,22]

Finally, an "excrescence drag," which accounts for additional parasite drag not yet considered in the modeling procedure including the drag of antennas, rivets, and other excrescences, was estimated. This drag was accounted for using a multiplier on the final drag buildup that increases drag by a percentage determined by engineering judgment. An excrescences multiplier of 1.075 was used for the SR-22, which resulted in a total parasite drag coefficient of 0.0171 at the point of minimum profile drag.

C. FLOPS Modeling

A FLOPS model was created to estimate the aircraft performance. FLOPS's built-in weight, aerodynamic, and propulsion models were calibrated to known data or other models using "override parameters," also known as "slope factors," to provide as realistic an estimation of performance as possible. The results from the aerodynamic modeling and VSP modeling were used to inform input values in FLOPS and modify internal FLOPS calculations using appropriate override parameters.

To create the final FLOPS aerodynamic model, the manual aerodynamic buildup performed at a single flight condition using the previously described procedure was compared to internal FLOPS aerodynamics calculations at that operating point. Appropriate values for span efficiency and percentages of laminar flow were input, and wetted areas were adjusted to match the VSP model using slope factors. Because FLOPS assumes that the aircraft has retractable landing gear, and most small general aviation aircraft including the SR-22 have fixed landing gear, the drag area determined from the aerodynamics buildup for the landing gear is input directly to the FLOPS file. Finally, appropriate values of the slope factors for the parasite drag and induced drag are selected to minimize the differences between the FLOPS drag model and the manual drag buildup.

A comparison of the drag polar determined by the manual buildup and the drag polar from the internal calculations in FLOPS is shown in Fig. 2. From the figure it is clear that the two polars exhibit little difference for C_L values between approximately 0.15 and 0.6. However, the inflection of the two curves is noticeably different, which causes greater deviations in predicted drag at lift coefficients outside of this range. The difference in inflection is likely due to the lack of detailed profile drag due to lift estimation inside of FLOPS. Because the curves only differ at fairly high or fairly low C_L values, the two drag predictions are very similar for the most common ranges of vehicle operation. The discontinuities in the manual drag polar buildup curve are a result of two unconverged, erroneous points in the induced drag output from XFLR5. The general trend of the drag polar is still evident even with these points and this trend was used to match the FLOPS internal aerodynamic calculations to the manual drag polar buildup.

FLOPS also estimates the weights of individual aircraft components, equipment, and subsystems based on geometric input parameters. The SR-22 POH, engine installation and operation manual, and delivered weight and equipment list were used to determine appropriate values for slope factors so that any known weights for the actual aircraft were matched exactly by the FLOPS model. However, because data was unavailable for all weights estimated by FLOPS, the internal estimations from FLOPS were used for these components or adjusted using engineering judgment to ensure that the known empty weight of the aircraft was matched.

Propulsion modeling was performed using FLOPS's internal engine modeling module ENGGEN.[25] This propulsion module generates an engine deck that describes the thrust and fuel flow rates for the engine-propeller combination across altitudes and Mach numbers. The input data required was determined from the POH and engine installation and operation manual. However, several parameters such as propeller integrated lift coefficient are not published in available information sources, so there was a fairly large degree of uncertainty in the propulsion system model. The values of the uncertain parameters were determined using

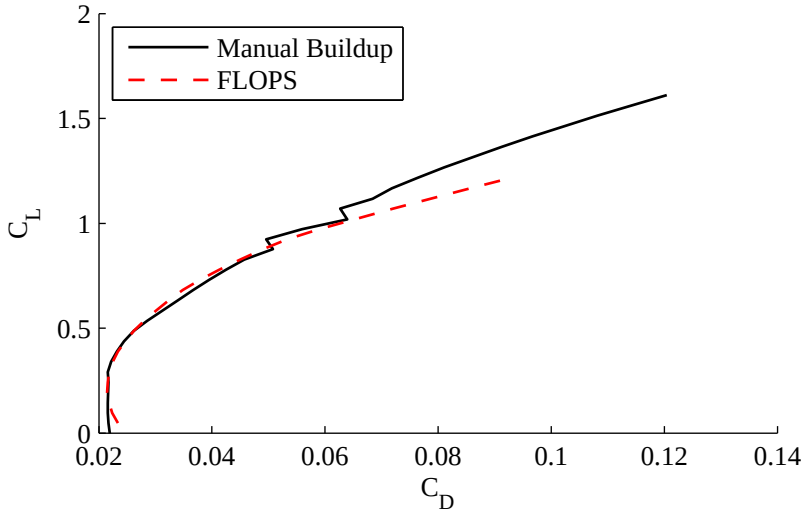

Figure 2. Comparison of SR-22 Drag Polars

a point performance calibration based on data from the POH once initial estimations of all necessary propulsion parameters were set, and wetted area, aerodynamic, and weight calibrations were made. This point performance calibration was used to ensure that accurate thrust values were calculated by the propulsion model.

Thrust was calibrated by matching estimated rate of climb (ROC) to known climb performance tabulated in the POH. The rate of climb is given by Eq. 4 when no acceleration is assumed.

$$\mathrm{ROC} = \frac{(T - D)\,V}{W} \tag{4}$$

POH data lists the rate of climb at a given velocity, altitude, and weight. Since the drag is "known" from the previous aerodynamic analysis, the only unknown remaining in Eq. 4 is the thrust. A climb schedule was entered into FLOPS so that direct comparisons between the FLOPS predicted rate of climb values and the POH values could be made for a range of altitudes. If discrepancies between the FLOPS data and the POH data for rate of climb were found, then adjustments were made to either the propulsion model (thrust) or the aerodynamic model (drag) or both. An iterative procedure was used to adjust unknown engine and propeller parameters such as integrated lift coefficient and activity factor until the error between the rate of climb predictions from FLOPS and the reported values from the POH was minimized. A comparison of the rate of climb values for the final model is shown in Table 1.

Table 1. Rate of Climb Comparisons

Altitude (ft)	FLOPS ROC (ft/min)	POH ROC (ft/min)	% Difference (%)
0	1412	1398	1.00
2000	1282	1279	0.24
4000	1151	1160	-0.78
6000	1028	1041	-1.27
8000	910	922	-1.28
10000	794	803	-1.17
12000	681	684	-0.39
14000	571	565	1.10
16000	466	446	4.58

The final step in propulsion modeling was to calibrate the fuel burn. Specific fuel consumption values and internal FLOPS slope factors for fuel flow rate were adjusted to match fuel burn rates at cruise. Comparisons of FLOPS predicted and POH reported fuel flow rates were made at several altitudes and power settings to ensure that the performance was matched in as many flight conditions as possible. Table 2 shows the comparisons between the predicted fuel flow rates from FLOPS and the actual fuel flow rates reported in the SR-22 POH for a range of altitudes and velocities, which represent many practical power settings.

Table 2. Fuel Flow Rate Comparisons

Altitude (ft)	Airspeed (knots)	POH Fuel Flow Rate (lb/hr)	FLOPS Fuel Flow Rate (lb/hr)	% Difference
2,000	186	139.8	144	2.92
2,000	179	125.4	128	2.03
2,000	167	102.0	103	0.97
6,000	184	120.6	121	0.33
6,000	177	108.6	108	-0.56
6,000	162	84.6	87	2.76
10,000	182	103.8	102	-1.76
10,000	168	84.6	81	-4.44
10,000	158	72.6	73	0.55
14,000	178	88.8	83	-6.99
14,000	171	79.8	77	-3.64
14,000	159	67.2	70	4.00

The final step in the baseline model calibration procedure was to compare aggregate mission performance from the FLOPS model to sample missions determined from the POH. Several sample missions from the performance charts in the POH that vary cruise altitude, speed, and distance were created and input into FLOPS to compare the performance. By setting the total mission fuel burn in the FLOPS model to the amount calculated from the POH performance charts for the mission, the resulting range of the aircraft computed by FLOPS was compared to the value determined from the POH performance charts.

Three sample missions for the SR-22 modeling were studied: 1) a high altitude, long range mission, 2) a low altitude, short range mission, and 3) a low altitude, long range mission. For each mission, the aggregate range was predicted with reasonable accuracy as is shown in Table 3. As expected, FLOPS predicts longer ranges than the conservative values obtained from POH performance tables.

Table 3. Mission Performance Comparisons

Mission	POH Range	FLOPS Range	% Difference
High Altitude, Long Range	600	621.9	3.65
Low Altitude, Long Range	250	255.5	2.20
Low Altitude, Short Range	87	93.6	7.59

D. Active Sizing Constraint Evaluation

To additionally verify the FLOPS model and to predict which constraints in the design of the SR-22 may have been active to size the aircraft, an optimization using FLOPS was performed. In this optimization, the wing size, thrust, and gross weight were used as design variables. An objective function was specified to minimize the gross weight of the aircraft for an 815 nmi mission with 45 min reserves flown at 8,000 ft and 180 knots while carrying 555 lb of payload subject to the following constraints:

- Takeoff field length on a standard day at sea level $\leq$ 1,594 ft to match the takeoff field length reported in the SR-22 POH

- Approach speed $\leq$ 79.3 knots to enforce the FAR-required stall speed of 61 knots[26] (since $V_{\text{approach}} = 1.3V_{\text{stall}}$)
- Rate of climb at 10,000 ft on a standard day at 108 knots and start of mission weight $\geq$ 803 ft/min to match the reported value in the SR-22 POH
- Rate of climb at cruise altitude $\geq$ 100 ft/min

The mission was selected from the "corner point" of the SR-22 payload-range diagram reported on the Cirrus website[17] where the maximum takeoff weight and maximum fuel weight constraints are both active. The rate of climb constraint at 10,000 ft was selected as a surrogate for a high altitude, hot day takeoff constraint.

The FLOPS model optimization produced the results shown in the first column of Table 4. The active constraints were found to be takeoff and rate of climb at altitude. Actual data for the SR-22 from the POH and the thrust value determined from the baseline SR-22 FLOPS model are shown in the second column. These values are compared to the optimization values via a percent difference in the final column. All values determined in the FLOPS optimization are within 3% of the actual values for the SR-22, which illustrates the accuracy of the baseline FLOPS model. At least some of these differences can be attributed to the FLOPS model's under-prediction of rate of climb at altitude. The rate of climb at 10,000 ft is underpredicted by 1.17% (see Table 1); by enforcing the rate of climb constraint at 10,000 ft to be the reported SR-22 rate of climb instead of the FLOPS model prediction, the thrust of the optimized aircraft must make up this additional 1.17% of thrust.

Table 4. Comparison of Optimization Results and the Baseline SR-22 Model

	Optimized FLOPS SR-22	Baseline FLOPS SR-22	Percent Difference
Gross Weight (lb)	3468	3400	2.0%
Wing Area (ft^2)	147.2	144.9	1.6%
Thrust (lb)	1120	1090	2.7%
ROC at 10,000 ft (ft/min)	806.6	803	0.4%
Stall Speed (knots)	59.1	59	0.2%
Takeoff Field Length (ft)	1593	1594	-0.1%

The active constraints in the optimization are the takeoff field length and rate of climb at 10,000 ft. It is interesting to note that with these two constraints active, the approach speed constraint was inactive, but converged to a value of 76.9 knots. This approach speed corresponds to a stall speed of just above 59 knots, which is nearly identical to the actual SR-22 stall speed. Determining the actual stall speed without the approach speed constraint being active further validates the SR-22 FLOPS model and indicates that Cirrus may have designed not to a 1,594 ft sea level takeoff field length, but rather a 59 knot stall speed.

III. Electric Aircraft Performance Analysis

With confidence established in the modeling method and a baseline aircraft model developed, electric aircraft models were developed using the modeling procedure, and the performance capabilities of these electric aircraft were studied and compared to the baseline. In this section we develop a Breguet-like range equation for battery electric aircraft and discuss several practical considerations on the resulting aircraft range. A notional fully electric SR-22-like aircraft is described using various technology assumptions, and the range capability of these aircraft is analyzed and compared to the baseline SR-22 using payload-range diagrams.

A. Electric Aircraft "Breguet" Range and Endurance

First-order estimates of electric aircraft range performance provide critical information to assess system feasibility. In order to quickly estimate the mission performance capability of electric aircraft, a Breguet-like range equation can be developed. Because electric aircraft experience no mass loss from fuel burn during the mission, a different approach based on energy consumption must be taken to develop this range

equation. The following derivation assumes a fully electric aircraft powered by an electric motor and battery system. While others have derived this equation,[27] presenting the derivation is useful for understanding the assumptions behind the final equation and the fundamental differences between electric and traditional fuel-burning aircraft.

The power required (to overcome drag) must be supplied by energy from the batteries. This power is produced via the electric motor system and propeller with efficiencies η_{elec} and η_{prop}, respectively. η_{elec} incorporates the efficiencies of all components from the batteries to the motor, including the efficiency of the batteries, motor controller, and motor. The power required can be expressed in terms of the overall efficiency, $\eta = (\eta_{\text{elec}})\,(\eta_{\text{prop}})$, and the time rate change of the energy available in the batteries, $\mathrm{d}E/\mathrm{d}t$, as

$$P_{\text{req}} = -\frac{\mathrm{d}E}{\mathrm{d}t}\eta \tag{5}$$

where the negative is necessary because the stored energy is reduced for a positive power output.

The differential time in Eq. 5 can be substituted for differential distance and velocity, and the resulting equation solved for $\mathrm{d}s$ as shown in Eq. 6.

$$\mathrm{d}s = -\frac{\mathrm{d}E}{P_{\text{req}}}V\eta \tag{6}$$

The required power can be expressed in terms of the drag and flight velocity, $P_{\text{req}} = DV$, which can be substituted into Eq. 7:

$$\mathrm{d}s = -\frac{\mathrm{d}E}{D}\eta \tag{7}$$

Eq. 8 results from multiplying Eq. 7 by W/W and assuming that the aircraft is in steady, level flight with the thrust aligned with the velocity vector so that $L = W$.

$$\mathrm{d}s = -\mathrm{d}E\frac{L}{D}\frac{\eta}{W} \tag{8}$$

Eq. 8 can be integrated over the total energy available in the batteries:

$$\int_0^R \mathrm{d}s = \int_{E_{\text{avail}}}^0 -\frac{L}{D}\frac{\eta}{W}\,\mathrm{d}E \tag{9}$$

For flight at a constant weight, lift-to-drag ratio, and overall efficiency, Eq. 9 simplifies to Eq. 10.

$$R = \frac{L}{D}\frac{\eta}{W}E_{\text{avail}} \tag{10}$$

The total energy available in the batteries can be expressed in terms of the battery energy density, u, the mass of the batteries, m_{bat}, and a measure of the percent charge of the batteries intended to be accessed during a typical mission, κ, as shown in Eq. 11.

$$R = \frac{L}{D}\frac{\eta}{W}\left[u\,(m_{\text{bat}})\,\kappa\right] \tag{11}$$

If the mass of the batteries is expressed in terms of the weight of the batteries, W_{bat}, and if a constant acceleration due to gravity, g, is assumed, then the "Breguet" range equation for electric aircraft can be expressed as Eq. 12.

$$R = \eta\frac{L}{D}\frac{W_{\text{bat}}}{W}\frac{u\kappa}{g} \tag{12}$$

For a given aircraft with a set total weight and set battery weight, range can be maximized by maximizing $\eta\,(L/D)$. Unlike traditional fuel-burning aircraft, electric aircraft do not have to preform a cruise climb to maintain a maximum lift-to-drag ratio due to their constant weight; additionally, to maintain a constant lift-to-drag ratio at a constant altitude and weight, a constant velocity is required. The constant altitude, constant speed flight required for maximum aircraft range is advantageous from air traffic control and pilot workload perspectives.

The "Breguet" endurance of electric aircraft can be developed in a similar manner as the range, and the resulting endurance equation is shown in Eq. 13.

$$N = \frac{\eta}{V}\frac{L}{D}\frac{W_{\text{bat}}}{W}\frac{u\kappa}{g} \tag{13}$$

This equation is related to the range by the velocity as $N = R/V$.

B. Other Electric Aircraft Range Considerations

In addition to a constant vehicle weight changing the optimum cruise profile, the use of electric propulsion systems has other impacts on the practical range achievable by these aircraft. These operational considerations center around the constant vehicle weight and federal aviation regulations (FARs) and are described in the following subsections.

1. Payload and Fuel Weight

There is a fundamental difference in the fuel types of full electrically-powered aircraft and traditional aircraft that impacts the operational effectiveness of these aircraft types for various payload weights. The operating weight of traditional aircraft depends directly on the amount of fuel carried. As fuel is added to traditional aircraft, payload often must be removed to keep the aircraft at or below the maximum takeoff weight. If larger payloads need to be carried, fuel can be removed from (or not added to) the aircraft. In contrast, removing electrical charge from batteries in electric aircraft will not impact vehicle weight. In order to practically achieve a similar trading of payload and fuel, batteries must be removed from or added to electric aircraft. Depending on the design of the aircraft, this trade may not be possible.

The payload vs. fuel weight trade can be shown on payload-range diagrams, which indicate the aircraft range achievable for a given payload weight. For traditional aircraft, these diagrams often indicate a maximum takeoff weight constraint where payload and fuel are directly traded. However, since there will likely not be a direct tradeoff between payload and battery weight in most future electric aircraft, payload-range diagrams for electric aircraft will have fundamentally different shapes than the traditional curves.

2. Reserves

Before performing a range analysis, the practical operation of the electric aircraft must first be considered. Federal Aviation Regulations (FARs) require that pilots operate aircraft with certain amounts of reserve fuel for the planned mission. These fuel reserves vary depending on the flight rules being used and the predicted weather conditions during the flight. There are two main categories of flight rules—visual flight rules (VFR) and instrument flight rules (IFR)—that require a different amount of reserve fuel. VFR requirements for aircraft state that during the day at least 30 minutes of reserve fuel must be carried, and 45 minutes of reserve fuel are required for night flights.[28] FAR requirements for IFR flight dictate that at least 45 minutes of reserve fuel must be carried.[29]

In order to comply with the FARs, electric aircraft will have to maintain a sufficient battery system charge to account for reserves, and any range analysis of electric aircraft should account for these reserves to provide a realistic comparison to existing aircraft. While maintaining a certain amount of reserve charge in the batteries will decrease the aggregate range predicted, these reserves may be synergistic with maintaining a long battery life at full capacity. Unlike traditional aircraft in which safety is the only advantage gained by keeping fuel in the tanks at the end of a flight, for batteries to maintain a long useful life, not all of the charge in the batteries should be used.

Since promotional materials published by Cirrus for the baseline SR-22[17] indicate the range capability of the aircraft with a 45 minute reserve, the analyses performed in this paper are computed with a 45 minute reserve segment performed at the appropriate cruise speed.

C. Electric SR-22-like Aircraft

As an initial study into the performance capabilities of electric aircraft, geometric, aerodynamic, and weight models of a fully electric variant of the SR-22 were created. Using the baseline SR-22 VSP model as a starting point, the nose size was slightly reduced to account for the smaller required volume for the electric motors and controllers. This nose size reduction resulted in a slightly reduced fuselage wetted area and, therefore, a reduction in parasite drag. Similarly, the electric motor requires much less cooling airflow, which nearly eliminates the cooling drag. At the reference cruise condition of 8,000 ft and 180 knots, the parasite drag coefficient reduction due to the reduced wetted area and cooling drag coefficient reduction were found to be 0.0004 and 0.0013, respectively. At these conditions the baseline aircraft has a total drag coefficient of 0.0216 while the electric variant has a total drag coefficient of 0.0199. The cooling drag of the electric variant was calculated assuming a temperature rise of the motor during operation of 60°C, a total electrical

system efficiency of 0.9, and all other relevant parameters from the original cooling drag model of the internal combustion engine remaining constant.

The electric SR-22-like aircraft has a different weight breakdown than the original SR-22 due to the propulsion system changes. The main difference is that the internal combustion engine, fuel system, and all other associated propulsion system components can be removed and replaced with electric motors, controllers, and batteries. The weight estimations of the propulsion system from the original SR-22 FLOPS model were used to estimate how much weight could be removed from the aircraft. This FLOPS model predicts a total propulsion system weight of 690 lb. Unusable fuel (18 lb) and engine oil (15 lb) are not included in the 690 lb total propulsion system weight and are not needed for the electric variant; therefore, an additional 33 lb can be removed from the aircraft, bringing the total propulsion system weight to 723 lb. However, not all components of the original propulsion system can be removed for the electric variant. Because the electric propulsion system still requires the propeller and cowl, the total weight that can be removed from the baseline SR-22 is 617 lb. The aircraft must then be equipped with the required components for a fully electric propulsion system. If a motor specific power of 3 hp/lb is assumed, a 103 lb motor is required to achieve 310 hp (the original engine horsepower). Therefore, there is a net operating empty weight decrease of 514 lb for the electric version of the SR-22 by removing the internal combustion engine and replacing it with an electric motor. This additional weight can be utilized for batteries or payload.

1. Motor Sizing Considerations

For the analysis presented above, the electric motor power was assumed to be equal to the actual SR-22; however, this may be a greater power than is actually required for an electric variant. Because electric motors, unlike internal combustion engines, experience no power lapse with altitude (presuming that cooling imposes no constraints), high altitude, hot day conditions may no longer be critical sizing constraints for propulsion system power. It should be noted that electric motors that drive propellers will still experience some *thrust* lapse with altitude due to the lapse of the propeller. This thrust lapse may still cause high altitude, hot day constraints to be critical sizing conditions, but less sea level static engine power will be required to match the same thrust at altitude with an electric motor than with an internal combustion engine.

If a critical design constraint of the SR-22 is a rate of climb at altitude (as was shown may be the case in Section II.D), the power of an electric motor can be set such that it meets the required shaft horsepower at the specified condition. By using propeller codes based on the propeller model in FLOPS, the required shaft power to produce the same thrust as the baseline SR-22 FLOPS model at 8,000 ft was found to be approximately 230 hp. While a conventional internal combustion engine would have to be rated at an even greater power to account for altitude lapse, an electric motor can be rated at 230 hp because it does not experience a power lapse with altitude. This implies that a motor size of approximately 25% less than the conventional SR-22 (rated at 310 hp) may be adequate for the electric variant of the SR-22 to meet critical sizing constraints.

This decrease in required power has impacts on system cost, weight, and performance. Generally speaking, electric motors with lower horsepower ratings will cost less than motors with higher horsepower ratings; therefore, reduced motor powers are desired from a cost standpoint. Additionally, reduced power requirements generally reduce the motor weight. In this case with a 230 hp motor, the motor weight can be reduced to 76.7 lb (assuming a 3 hp/lb), which allows for over 26.6 lb more of payload or battery weight in the aircraft. This extra weight savings could increase range or allow for greater payloads weight.

The performance of the aircraft with a smaller motor will also be impacted. Traditional internal combustion engines achieve improved low altitude performance "for free" when they are sized to high density altitude constraints. The conventional SR-22 can achieve 310 hp at sea level, which improves performance metrics such as takeoff distances and rate of climbs. An electric motor sized to 230 hp will not be able to achieve the same level of performance at altitudes lower than that to which it was sized. Therefore, while a single rate of climb constraint may be satisfied with 25% less power, other constraints may become critical in the sizing process. It should also be noted that if a 310 hp electric motor is used, the aircraft will have improved point performance capability at altitude when compared to the conventional SR-22. The use of electric motors will therefore introduce new design tradeoffs between low altitude point performance, high altitude point performance, mission performance, and cost.

D. Technology Assumptions

Due to the constant evolution of electrical system technologies, there is uncertainty in the level of battery, motor, and motor controller technologies that will be available for future on-demand aircraft. Before analyzing the performance of electric aircraft, the technological assumptions behind the electric motors, motor controllers, and batteries must be set. We have divided these technology assumptions into three time frames: 2015, 2035, and 2050. These technology level estimates are based on the authors' survey of existing and forecasted hardware being developed at companies researching in this area. All the 2015 technology levels have already been demonstrated in laboratory tests and are at a Technology Readiness Level (TRL) of at least 6, which indicates readiness for integrated flight testing with likely availability within the next few years. The 2035 values were derived from linear extrapolations of the improvement rate over the past 20 years. These values are likely conservative due to potential non-linear improvement rates caused by discontinuous technology jumps that may be achieved through significant investment for automotive applications and government funding of advanced batteries. It is possible that emerging battery technologies such as Envia may result in reaching 400 W-hr/kg by the 2015 date.[30] Advanced motors that utilize such approaches as Halbach arrays, are already achieving specific power of 5 hp/lb in lab tests. Researchers are currently studying novel approaches of tailoring custom magnetic fields to such motors to achieve a factor of three improvement in their torque for the same mass. Therefore, it is conceivable that advanced electric motors could achieve specific powers of 10 to 15, even in the near-term. However, the fundamental logic of the technology level selection was to evaluate three states of electric propulsion that vary from current, to dramatically improved levels.

Table 5 summarizes these assumptions, which are important in determining the total energy that can be stored in the batteries and the fraction of that energy that can be converted into useful flight power. The following analyses use these technological assumptions unless otherwise stated.

Table 5. Technology Assumptions

	Technology Year		
	2015	2035	2050
Motor Peak Specific Power (hp/lb)	4	6	12.5
Motor Nominal Specific Power (hp/lb)	3	4.5	9.375
Motor Efficiency without Gearbox	0.95	0.97	0.98
Motor Efficiency with Gearbox	0.925	0.95	0.97
Controller Specific Weight (lb/hp)	0.05	0.05	0.05
Controller Efficiency	0.98	0.99	0.99
Battery Specific Energy, <5C (W-hr/kg)	200	600	1200
Battery Specific Energy, >5C, <20C (W-hr/kg)	150	450	900
Battery Specific Energy, >20C, <60C (W-hr/kg)	100	300	600
Battery Efficiency	0.98	0.98	0.99

E. Range Comparisons

The Breguet range of electric and conventional SR-22-like aircraft can be compared by using Eq. 12 for electric concepts and the traditional Breguet range equation for reciprocating engine, propeller-driven aircraft given in Eq. 14.

$$R = \frac{\eta_{\text{prop}}}{SFC}\frac{L}{D}\ln\left(\frac{W_{\text{initial}}}{W_{\text{final}}}\right) \tag{14}$$

By performing simple analyses using Eqs. 12 and 14, the feasibility of modifying existing aircraft to use fully electric propulsion systems can be studied. If simplified Breguet-like analyses indicate considerably lower range than conventional aircraft, then studies can be performed to determine what technology levels must be reached before feasibility can be achieved. Alternatively, if these analyses indicate near-equivalent or improved ranges for electric aircraft, then more detailed studies should be performed to determine the range more accurately.

The results from the simplified range analysis for the electric SR-22-like aircraft with a 45 minute reserve using 2015 technology levels are shown in Fig. 3. This figure shows two different pairs of payload range

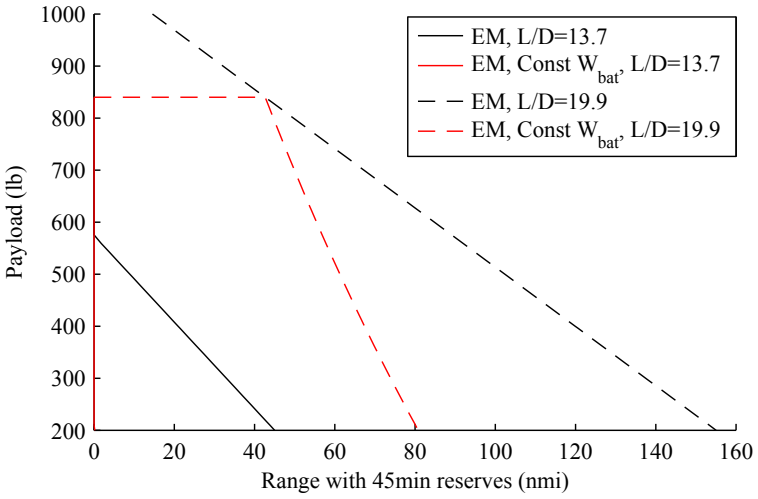

Figure 3. Electric SR-22-like Aircraft Payload Range Diagram

curves for the version of the SR-22 driven by an electric motor (EM): 1) constant battery weight and 2) variable battery weight. For each of these cases, two different operating conditions are shown, which are defined by different lift-to-drag ratios. The $L/D = 19.9$ curves represent operation at a maximum L/D, which corresponds to a velocity of 128 knots at 8,000 ft. The $L/D = 13.7$ curves correspond to operation at 8,000 ft and 180 knots. For the variable battery weight curves, a constant takeoff weight of 3400 lb (the maximum takeoff weight for the SR-22) was maintained by trading payload weight for battery weight. It is assumed for the variable battery weight cases that when the payload weight increases, batteries are removed from the aircraft so that the battery weight decreases. Similarly, as payload is decreased, batteries are added to maintain a constant takeoff weight. Because it may not be practical to add and remove batteries from the aircraft, a case with constant battery weight was also studied. For this case, the battery weight was set to 745 lb so that when 840 lb of total payload is carried—four passengers and baggage at 210 lb each—the takeoff weight is 3400 lb. These curves are cut off at a payload weight of 840 lb because any higher payload weights would lead to a takeoff weight above the maximum of 3400 lb.

It is clear that the range capabilities for the aircraft shown in the figure are not very practical. Only the variable battery weight case operated at the maximum lift-to-drag ratio (which corresponds to a relatively slow speed) has the capability to fly over 100 nmi with FAR reserves. If higher speeds are desired, range capability suffers greatly, as can be seen by comparing either the two black lines or the two red lines for variable or constant battery weight, respectively. In fact, all of the battery capacity must be saved for the reserve segment for the higher speed operation if the battery weight is held constant, which gives the aircraft zero practical range in that case. These results indicate that within the next few years, electric aircraft that are simply modifications to existing airframes will likely need to operate at relatively slow speeds for short ranges.

In order to compare the range capability of the electric SR-22-like aircraft with conventionally-powered aircraft, Eq. 14 was used to determine the range of the baseline SR-22-like aircraft and the results were plotted on the payload range diagram shown in Fig. 4. This figure shows two cases for an SR-22 driven by a conventional internal combustion engine (ICE) in addition to the four cases previously described for the electric variant. The two curves for the conventionally-powered aircraft represent operation at different lift-to-drag ratios, which are indicated in the figure. The $L/D = 18.7$ curve represents operation at a maximum L/D, which corresponds to an initial velocity of 128 knots at 8,000 ft. The $L/D = 11.7$ curves correspond to operation at an initial velocity of 128 knots at 8,000 ft. Because these curves assume constant L/D operation and the weight of the aircraft changes during flight, either the altitude or velocity or both will change throughout the flight. For these curves, the propeller efficiency (η_{prop}) was assumed to 0.85 and the specific fuel consumption (SFC) was assumed to be 0.5086 lb/(hp-hr).[31]

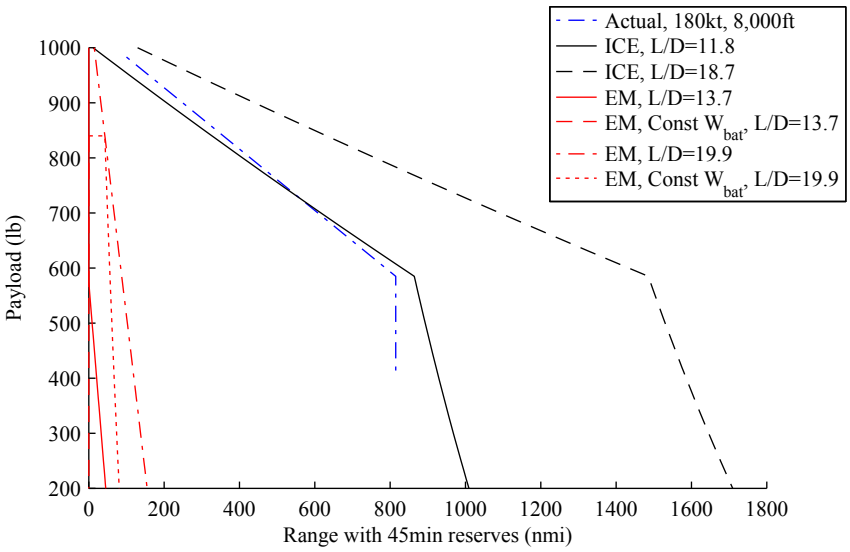

Figure 4. SR-22-like Aircraft Payload Range Diagram: Conventional Propulsion and 2015 Electric Propulsion Technologies

In addition to the two payload range curves generated from the Breguet range equation, a curve representing the range capability of an SR-22 operated at a constant speed of 180 knots and constant altitude of 8,000 ft is shown with a blue line in Fig. 4 as a point of comparison. The data for this curve was taken from the Cirrus website, and can be considered the "actual" range capability of the aircraft.[17] It is important to note the differences in assumptions of the Breguet range equation and the flight profile used for the SR-22 data from Cirrus. The Breguet range equation assumes flight at a constant lift-to-drag ratio; a flight at constant altitude and constant speed for a conventional aircraft where the weight changes during flight will be flown with a variable C_L and, therefore, a variable L/D. This difference in flight profiles leads to differences in the range calculations and explains the different shapes of the blue and black payload range curves in Fig. 4. The blue curve is cut off at a payload weight of 400 lb because the data given on the Cirrus website only indicates the range capability from 400 lb of payload to 1,000 lb of payload. Because the line from 400 lb to 585 lb of payload is vertical, Cirrus appears to take no extra range credit as payload is off loaded from the maximum takeoff weight with full fuel tanks, which is a different assumption than was made for the curves generated by the Breguet equation.

Figure 4 illustrates the very large difference in range capability between an electric aircraft with 2015-era technologies and current internal combustion engine-driven aircraft. For many payloads, the SR-22 has the ability to fly over 1,000 nmi farther than the electric aircraft created from simply exchanging propulsion systems. This massive range capability gap indicates a serious hurdle in creating practical electric aircraft from simple modifications of existing, tried-and-true airframes in the near future.

Also as can be seen in Fig. 4, the electric aircraft curves exhibit a noticeably steeper slope than the conventional propulsion system curves. This slope difference is indicative of the different energy densities of the two types of fuel. The low energy density of batteries means that adding 1 lb of battery weight does not improve range as much as adding 1 lb of aviation fuel.

In order to study the influence of projected technological increases, similar payload range diagrams were generated using 2035 and 2050 technology assumptions. Figures 5 and 6 show the payload range diagrams for projected 2035 and 2050 technologies, respectively. Both of these figures indicate a much improved range for electric aircraft compared to 2015 technologies with even greater range than the current conventional technology at high payload weights. However, at low to moderate payload weights, even projected 2050 electric propulsion technologies in a slightly modified version of current airframe are not quite sufficient to match current capabilities *across all payload weights*. It is important to note that these electric aircraft may be better-suited for some missions (in this case higher payloads) than others.

The slopes of the lines for the electric aircraft are less steep than those in Fig. 4, which indicates that more traditional tradeoffs between payload and range can be expected in electric aircraft with increased

battery energy densities and efficiencies. However, the slopes of the electric payload range curves are still steeper than the conventional aircraft. This steeper slope causes the electric variant to be capable of longer ranges than the conventional SR-22 when high payloads are required, but shorter ranges when carrying low payloads. Additionally, the ranges achievable with both 2035 and 2050 technologies are practical for many flights that are traditionally taken with smaller general aviation aircraft, including training flights. While the range performance may not match current capabilities across all payload weights, electric aircraft that are simple modifications to existing airframes may become a perferred means of flight due to the lower operating costs, noise, emissions, and other benefits.

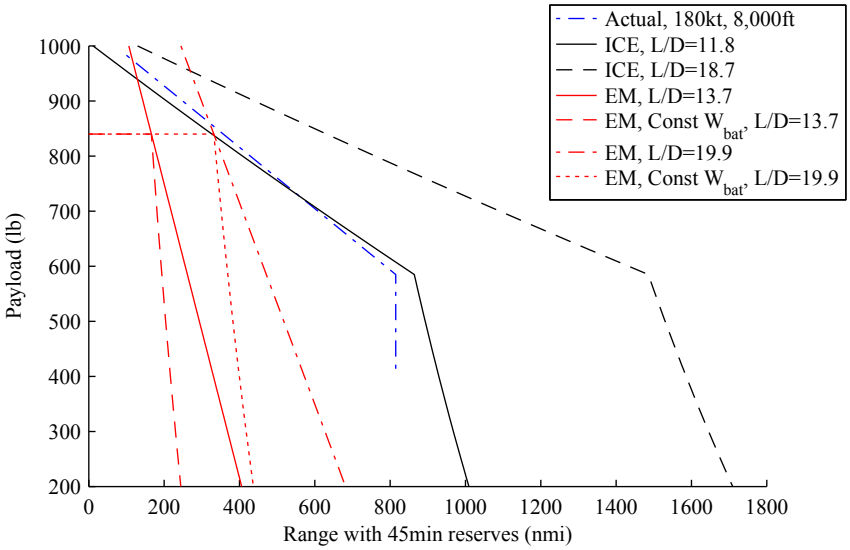

Figure 5. Conventional and Electric SR-22-like Aircraft Payload Range Diagram with Projected 2035 Technologies

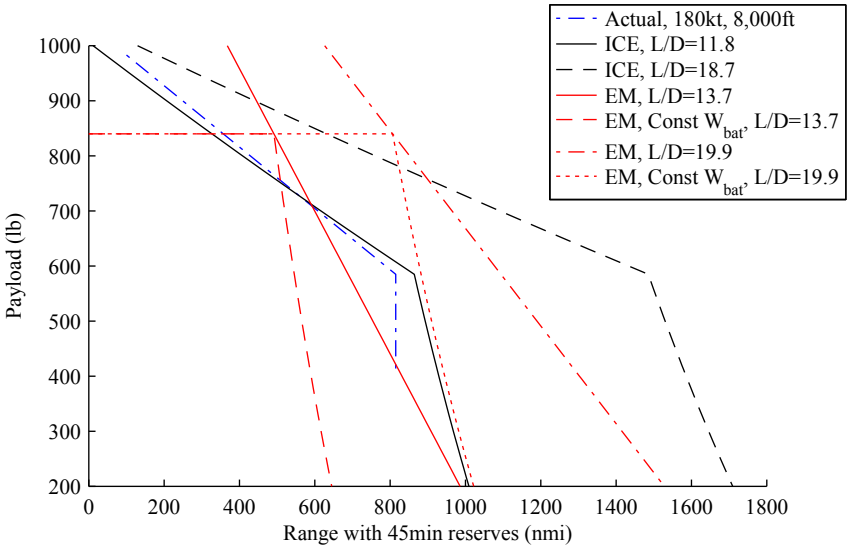

Figure 6. Conventional and Electric SR-22-like Aircraft Payload Range Diagram with Projected 2050 Technologies

IV. Electric Aircraft Sizing

As discussed in Section III, fully electric aircraft derived from simple modifications to existing small general aviation airframes are unlikely to be capable of practical operational use in the near term. In this section, we evaluate the practicality of developing aircraft that are appropriately sized to realistic mission lengths. Fully electric aircraft that are larger than conventional smaller general aviation aircraft may be capable of achieving practical range performance in the near term. In this section, electric aircraft sizing logic is developed and the approach is used to estimate the required sizes for fully electric aircraft to meet proposed on-demand missions for the 2015, 2035, and 2050 time frames.

A. Sizing Logic

1. Gross Weight Determination

The electric aircraft Breguet range and endurance equations, Eqs. 12 and 13, can be used to estimate the necessary aircraft size to meet a specified range with reserves corresponding to a specified cruise velocity (V) and a specified percentage of the total available battery energy (κ). Presuming values for lift-to-drag ratio (L/D), overall efficiency (η), and battery energy density (u), the remaining task is to determine the required weights.

The weight breakdown for electric aircraft powered by batteries is given by Eq. 15,

$$W = W_{\text{empty}} + W_{\text{bat}} + W_{\text{payload}} \tag{15}$$

where the payload weight includes the crew. The empty weight and battery weight can be expressed with weight fractions as,

$$W = \left(\frac{W_{\text{empty}}}{W}\right) W + \left(\frac{W_{\text{bat}}}{W}\right) W + W_{\text{payload}} \tag{16}$$

which can be solved for the weight in terms of the weight fractions and payload weight as shown in Eq. 17.

$$W = \frac{W_{\text{payload}}}{1 - (W_{\text{empty}}/W) - (W_{\text{bat}}/W)} \tag{17}$$

Eq. 17 can be solved iteratively as is done in conventional aircraft sizing to determine the required aircraft gross weight.

The empty weight fraction (W_{empty}/W) can be found from historical regressions as with traditional sizing. However, the authors are unaware of weight fraction regressions for small electric aircraft in the same class that can be used as a reference. Typical single engine general aviation equations could be employed; however, the electric motor and controller weight is expected to be considerably less than a traditional internal combustion engine. Additionally, the "fuel" weight of electric aircraft (at least in the near-term) will likely comprise larger percentages of the aircraft gross weight than typical general aviation aircraft because batteries are currently heavier than aviation fuel on a per unit energy basis. Therefore, it is likely that these electric aircraft will have empty weight fractions less than typical single engine general aviation aircraft. However, in the absence of better data on existing electric concepts, single engine general aviation aircraft empty weight fractions are used in this study as an estimate for single-motor electric aircraft.

Another difficulty in using Eq. 17 is determining the "battery weight fraction" (W_{bat}/W). This fraction is not directly analogous to the fuel weight fraction in traditional sizing. However, the battery weight fraction necessary for a set range and/or endurance can be solved for directly in the electric Breguet range and endurance equations (Eqs. 12 and 13).

For endurance segments flown at a constant velocity, the Brequet range and endurance equations (Eqs. 12 and 13) can be related by the velocity:

$$R = NV \tag{18}$$

Therefore, the range associated with an endurance segment flown at constant velocity can be found from Eq. 18. If a vehicle is to be sized to both a specified range and an additional endurance requirement, the range and endurance can be represented as an aggregate range as shown in Eq. 19.

$$R_{\text{total}} = R_{\text{design}} + N_{\text{design}} V_{\text{design}} \tag{19}$$

The required battery weight fraction can be determined by substituting the total range into the electric Breguet-like equation and solving for the battery weight fraction as shown in Eq. 20.

$$\frac{W_{\text{bat}}}{W} = \frac{\left(R_{\text{design}} + N_{\text{design}} V_{\text{design}}\right) g}{\eta \left(L/D\right) u \kappa} \tag{20}$$

The reserve fuel margins required in the FARs specify that sufficient reserve fuel to fly an endurance segment (expressed as a time in minutes) at a "normal cruising speed" must be carried. Equation 20 can therefore be used to size an aircraft for a practical range (R_{design}) that accounts for required reserves (N_{design}).[28,29]

While Eq. 20 could be used alone to achieve a basic sizing estimate for an electric aircraft, additional calculations should be performed to account for battery health considerations. Maintaining the health of some battery types requires that the batteries not be completely depleted of charge and/or recharged to full capacity. To account for this, the value of the variable κ in Eq. 20 can be varied. For example, if the last 20% of the battery should be preserved in order to prolong battery life, the value of κ used to determine the battery weight fraction could be set to 0.8. However, with this approach, the aircraft would be sized such that only 80% of the battery capacity would be expended during the design mission range and full reserve segment. In many cases, this approach may result in an overly conservative sizing estimate because with proper flight planning, the reserve fuel often is not required to safely complete a mission. If no reserves are needed for a flight, then the energy required for the reserve segment remains in the battery at the end of the mission. This remaining charge can constitute some or all of the energy margin required to maintain good battery health. In the example case when the last 20% of the battery should be preserved, battery health would not suffer if 80% of the battery charge were used in the design range segment. The reserve segment can be accounted for with some or all of the last 20% charge since reserves are likely to be unneeded for successful mission completition.

To size the aircraft while accounting for battery health, we first use Eq. 20 with $\kappa = 1$ to calculate the battery weight fraction. The aircraft range is then computed with Eq. 12 based on the calculated battery weight fraction and an appropriate value of κ to preserve a specified amount of charge in the batteries. If the resulting range calculated from Eq. 12 with this procedure is less than the design range, the implication is that battery health concerns are more constraining than FAR fuel reserve requirements. To determine the appropriate battery weight fraction in this case, only the design range (*not* the total range including reserves) and an appropriate value of κ are used to calculate the battery weight fraction. This is done by solving Eq. 12 for the battery weight fraction as shown Eq. 21.

$$\frac{W_{\text{bat}}}{W} = \frac{R_{\text{design}} g}{\eta \left(L/D\right) u \kappa} \tag{21}$$

This procedure is summarized in Algorithm 1.

2. Wing and Motor Power Sizing

After determining the required aircraft gross weight, the associated wing size and motor power required for a set of point performance constraints can be determined. In this paper, we enforce the stall speed and high-altitude climb constraints identified in Section II.D as potential sizing constraints for the SR-22. We acknowledge that these constraints are not necessarily active for all designs and may lead to undersizing the wing and/or motor. However, these two constraints were shown to be potential sizing points for the SR-22, and can provide at least a lower bound on the wing size and motor power that are necessary.

The wing size is assumed to be set by the FAR stall speed requirements for single-engine aircraft certified under FAR 23, which specify a maximum stall speed of 61 knots.[26] For a presumed maximum lift coefficient, the wing size can be estimated directly from this stall speed.

The motor power requirement is estimated by a rate of climb constraint at altitude since our analysis has shown that this constraint may be active for the SR-22. The rate of climb equation, Eq. 4, can be used to estimate the power by expressing the thrust in terms of the power as $T = P\eta_{\text{prop}}/V$. The best rate of climb velocity and associated drag at that velocity can be approximated by presuming the aircraft drag polar. With this information, the required motor power can be approximated.

Algorithm 1 Battery Weight Fraction Calculation

1:
$$\left(\frac{W_{\text{bat}}}{W}\right)_1 = \frac{\left(R_{\text{design}} + N_{\text{design}} V_{\text{design}}\right) g}{\eta \left(L/D\right) u \left(1\right)}$$

2: For $\kappa < 1.0$:
$$R_1 = \eta \frac{L}{D} \left(\frac{W_{\text{bat}}}{W}\right)_1 \frac{u\kappa}{g}$$

3: **if** $R_1 \geq R_{\text{design}}$ **then**

4:
$$\frac{W_{\text{bat}}}{W} = \left(\frac{W_{\text{bat}}}{W}\right)_1$$

5: **else**

6:
$$\left(\frac{W_{\text{bat}}}{W}\right)_2 = \frac{R_{\text{design}} g}{\eta \left(L/D\right) u\kappa}$$

7:
$$\frac{W_{\text{bat}}}{W} = \left(\frac{W_{\text{bat}}}{W}\right)_2$$

8: **end if**

B. Initial Sizing Results

Since our previous analysis has shown that simple modification of propulsion systems to an existing airframe will likely not provide a practical aircraft in the near term, the sizing logic mentioned above was implemented to determine the aircraft size required to meet projected on-demand missions. As with the technology assumptions, these missions are divided into three different years: 2015, 2035, and 2050. For each year, different design ranges and velocities are required to meet a practical on-demand mission.[6] A summary of the required mission parameters can be seen in Table 6.

Table 6. On-demand Mission Specifications

	Year		
	2015	2035	2050
Design Range (miles)	200	300	500
Design Range (nmi)	173.8	260.7	434.5
Design Velocity (mi/hr)	150	200	250
Design Velocity (knots)	130.3	173.8	217.2
Reserve Time (min)	45	45	45

Three aircraft—one for each year specified—were sized using the information in Table 6. An aircraft based on the electric variant of the SR-22 was used to provide guidance for the lift-to-drag ratio and drag polar used in the sizing. A lift-to-drag ratio of $L/D = 18.75$, propeller efficiency of $\eta_{\text{prop}} = 0.85$, and a maximum fraction of the batteries to use of $\kappa = 0.8$ were selected. This L/D value is approximately the lift-to-drag ratio of the modified electric SR-22-like aircraft if operated at 150 mph. The battery energy densities used in the sizing were selected from the technology assumptions in Table 5 for the three different years. A drag polar of the form $C_D = 0.0212 + C_L^2/\left(\pi \left(0.71\right) \left(10.26\right)\right) - 0.008 C_L$ was assumed based on the drag polar of the electric variant of the SR-22. The power was estimated with a rate of climb constraint of 800 ft/min at an altitude of 10,000 ft to match the point-performance capability of the SR-22 at that point. The initial sizing results for aircraft designed to carry 840 lb payloads using a single-engine general aviation empty weight fraction regression ($W_e/W_0 = 2.36 W_0^{-0.18}$)[19] are shown in Table 7.

As indicated in Table 7, the gross weight of the aircraft for the 2015 time frame is considerably higher than traditional general aviation aircraft. For certification under FAR 23 in the normal or utility categories,

Table 7. Initial Sizing Results

	Technology Year		
	2015	2035	2050
Gross Weight (lb)	11,170	3,575	3,035
Empty Weight (lb)	4,924	1,935	1,691
Battery Weight (lb)	5,406	801	503
Wing Area (ft^2)	445.5	142.6	121.0
Motor Power (hp)	548	175	149

the maximum takeoff weight allowable is 12,500 lb,[32] which is only approximately 1,300 lbs heavier than the etimated 11,170 lb gross weight. This large gross weight is outside the bounds of the single-engine general aviation empty weight fraction regression equation that was used in the calculations; therefore, it is uncertain whether the resulting empty weight fraction of approximately 0.44 for the 2015 era aircraft is an appropriate value because it extrapolates the historical trends. While this weight fraction is lower than traditional single-engine general aviation aircraft, it may be reasonable because of the reduced weight of electric motors when compared to internal combustion engines and the higher gross weight of this sized concept.If a higher weight fraction is required, the resulting gross weight would increase.

The high required gross weight of the 2015 era aircraft requires a very large wing to maintain compliance with FAR stall speed requirements for single-engine aircraft. If the wing maintains the same aspect ratio as the baseline electric SR-22-like aircraft, an unpractical span of over 67 ft is required. The very large wing also makes the power requirement calculation suspect due to the changes in the drag polar that would occur with a larger reference area. Ultimately, the very large required size of the aircraft in 2015 brings into doubt the practicality of creating fully electric aircraft *that are simple modifications of existing airframes* in the near future.

However, the required sizes of aircraft for the 2035 and 2050 technology assumptions are very practical. These aircraft are either slightly heavier or slightly lighter than the baseline SR-22 (which has a gross weight of 3400 lb), and the required wing sizes are also close to the baseline SR-22 (144.9 ft^2). These sizing results indicate similar conclusions as those found with the payload-range diagrams above (Figs. 5 and 6): with technology advances—specifically battery energy density—small, fully-electric aircraft that are simple modifications of existing airframes can become a practical means of transportation.

C. Sizing Sensitivity Studies

In order to study how various parameters influence the resulting size of electric concepts, several sensitivity studies were performed. For each of these studies, the technology assumptions for the three different technology years defined above are used unless otherwise stated. Motor efficiencies were assumed to be the efficiency with a gearbox and battery energy densities were selected as the values for applications that require less than a 5C rating. Also for each study, the variations of the parameters indicate the sensitivity in a partial derivative sense: all other variables are held at constant values while varying the single parameter. These sizing sensitivity studies use the Breguet-based sizing logic described above, which considers only cruise and reserves and neglects other segments such as takeoff or climb. The results are presented assuming 45 min of reserves in addition to the baseline ranges for each technology year as defined in Table 6, while never using more than 80% of the available battery charge for the design range ($\kappa = 0.8$). A four-passenger payload of 840 lb and a propeller efficiency of 0.85 are assumed. Finally, the results for each study only show gross weights of up to 12,500 lb because the certification of general aviation aircraft under FAR 23 limits the maximum takeoff weight of these aircraft to 12,500 lb in the normal and utility categories.[32]

1. Sensitivity About A Single Baseline

For the first set of sensitivity studies, the concepts sized in the preceding section for each of the three technology years were used as baselines about which the technological and mission assumptions were perturbed. The lift-to-drag ratio, battery energy density, total electrical system efficiency, design payload weight, and design range were each varied about the baseline design point and the results are shown in Fig. 7. The three

columns of this chart correspond to the three different technology years and the y-axis of each plot is the required aircraft gross weight in thousands of pounds. The baseline designs listed in Table 7 are denoted with an asterisk on each plot, with the baseline from the appropriate year corresponding to the columns.

The 2015 plots indicate very strong relationships between required gross weight and lift-to-drag ratio, battery energy density, and design range. There is a very distinct "knee" in the 2015 energy density curve at approximately 450 W-hr/kg. At lower energy densities, the required vehicle weight increases drastically with small changes in energy density and at higher energy densities there is a very small change in vehicle weight with energy density. At an energy density of 450 W-hr/kg, the required aircraft gross weight is approximately 3480 lb, which is very close to the weight of the baseline SR-22. This chart indicates a "technology frontier" in energy density may be reached if 450 W-hr/kg batteries can be produced for vehicles with a 200 mile range.

There is also a strong relationship between the required vehicle weight and the lift-to-drag ratio in the 2015 time frame. While this curve does not show as distinct an inflection point as the energy density, there is still a noticeable inflection in the curve near $L/D = 25$. This indicates that even if battery technology does not progress beyond the 200 W-hr/kg assumption, vehicle weights could still decrease to about 5,900 lb if the lift-to-drag ratio were increased to 25. Increasing L/D beyond 25 would still be beneficial, but would result in diminishing returns.

A moderate relationship between required gross weight and total electrical system efficiency are shown for the 2015 time frame. If the efficiency were increased by approximately 7% to 0.95, the gross weight could be reduced by approximately 17%. While improving the efficiency would help reduce the required aircraft size, the changes in gross weight with this parameter are less significant than changes in L/D or energy density.

The final two rows of Fig. 7 indicate changes in vehicle size with changes in the sizing mission. The required vehicle gross weight reduces nearly linearly with reduced payload weight—for every pound of payload decreased, the required gross weight of the aircraft decreases by approximately 6 to 7 lb. The trend of gross weight with design range is far from linear. The trend over all FAR 23-certifiable gross weights has increasing slope with range. If the required range is decreased by 25% from the baseline value of 200 miles, the required gross weight is reduced by approximately 35%. These final two rows indicate that in the near term, fully electric aircraft that are simple modifications of existing airframes will be most practical for missions with low payloads requiring short ranges.

The trends for 2035 and 2050 era technologies and missions do not indicate changes in gross weight that are as drastic as those observed in the 2015 time frame with the exception of battery energy density. The inflection points for the 2035 and 2050 energy density curves are very evident, but shifted to the right as compared to the 2015 time frame. For the 2035 baseline this inflection point occurs slightly higher than an energy density of 500 W-hr/kg, while for the 2050 time frame, the inflection point is seen at approximately 700 W-hr/kg. These results indicate that increasing battery energy density is the highest priority for making practical fully electric aircraft.

In contrast to the 2015 trend, the variation of gross weight with lift-to-drag ratio in the 2035 and 2050 time frames is much less dramatic. As long as L/D is greater than approximately 15, only small improvements in vehicle gross weight can be achieved by further increases. Also, there is very little variation of vehicle gross weight with the electrical system efficiency for the 2035 and 2050 time frames—at most a 5% increase from the 2035 baseline value to an ideal system with efficiency of 1.0. These results indicate that in the far future, very large changes in L/D and electrical system efficiency will be required to see even moderate change in gross weight.

Changes in the sizing mission and payload also show reduced impacts in the 2035 and 2050 time frames when compared to 2015. For each pound of payload decreased, the required gross weight only drops by about 3 lb for both the 2035 and 2050 time frames, which is approximately half as much change in gross weight as the 2015 time frame. Gross weight changes with changes in design range are still quite significant in 2035, but are considerably less strong in the 2050 time frame.

2. Sensitivity About Various Baselines

To view the importance of different baseline designs on the sensitivities, another set of sensitivity studies was performed using various baseline aircraft for each technology year. These new baselines were formed by using two different values of the lift-to-drag ratio, battery energy density, and empty weight fraction. These three parameters were selected because the results from the initial set of sensitivity studies indicated that

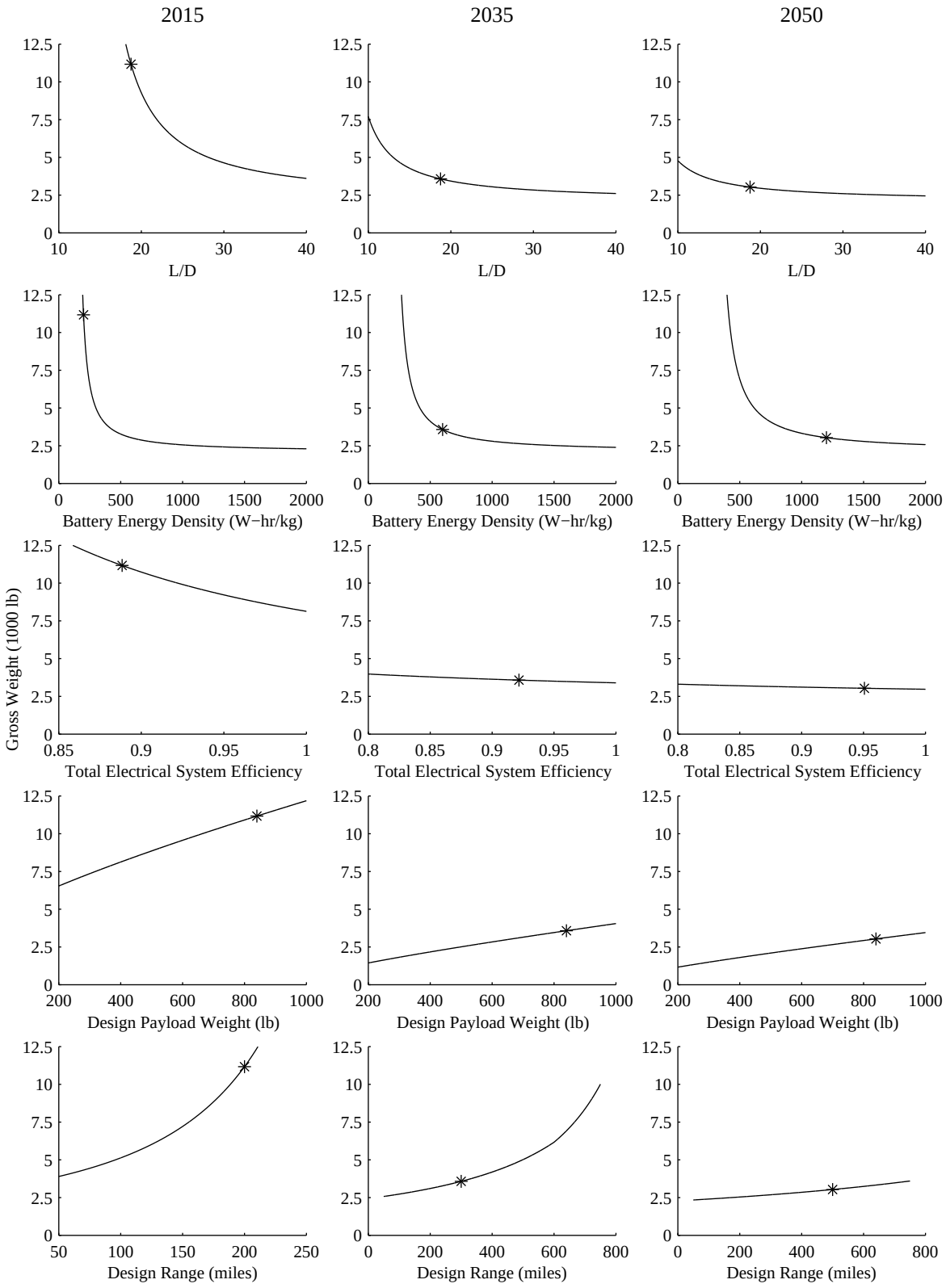

Figure 7. Sizing Sensitivity Study about Baseline Design for Three Technology Years

L/D and battery energy density were the most important parameters and the large vehicle size required for the 2015 time frame extrapolated trends in the empty weight regression equation. It is important to note that the empty weight fractions for these studies are held constant at particular values whereas the first set of studies used regressions of empty weight fraction versus gross weight. The baseline L/D values were selected as 15 and 25 and the baseline empty weight fractions were selected as 0.45 and 0.65. The baseline energy densities were selected from the information in Table 5, using the two highest energy density assumptions for the appropriate years. The results of these studies are shown in Fig. 8.

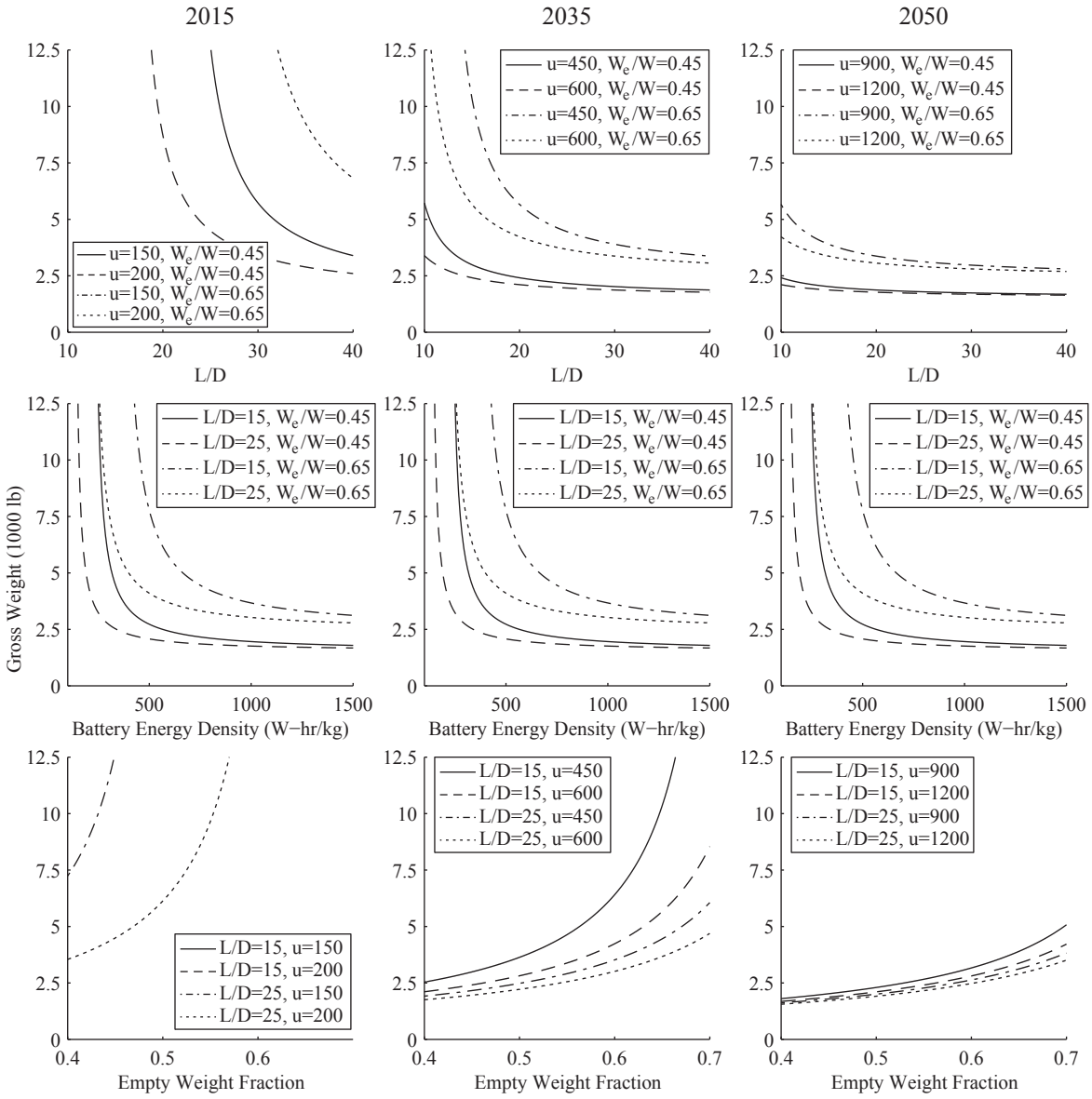

Figure 8. Sizing Sensitivity Study About Various Baseline Designs

As with Fig. 7, the columns of Fig. 8 indicate different technology years and the rows correspond to different parameters. Each plot contains four different curves corresponding to all combinations of the other two values of the two other baseline parameters. For example, for the 2015 time frame the energy density plot in the second row and first column has two lines that correspond to $L/D = 15$—one for each of the two empty weight fractions—and two lines corresponding to $L/D = 25$, each paired with a different empty weight fraction. However, four curves are not visible on every plot (i.e., the 2015 era L/D and empty weight fraction plots) because no feasible designs with gross weights less than 12,500 lb are possible for some baseline cases.

In the 2015 time frame, there are very steep trends in required gross weight with all three parameters for all different baselines. In the lift-to-drag ratio sensitivity plot, only three curves are visible because the curve corresponding to an empty weight fraction of 0.65 and a battery energy density of 150 W-hr/kg requires gross weights of greater than 12,500 lb for all the L/D values shown. The lowest curve on the plot with $W_e/W = 0.45$ and $u = 200$ W-hr/kg is almost identical to the curve shown in Fig. 7 for the 2015 variation of gross weight with lift-to-drag ratio. As the energy density is decreased or the empty weight fraction is increased, the "knee" in the L/D sensitivity curve is pushed toward higher lift-to-drag ratios. It is clear that lower the empty weight fractions and higher battery energy densities are most advantageous.

In the 2015 empty weight fraction plot, only two curves are visible that each correspond to lift-to-drag ratios of 25. This indicates that lift-to-drag ratios of 15 are impractical for both of the assumed baseline energy density levels. (The same trend can be observed from the asymptotic nature of the L/D curves in the top left plot.) The slopes of each of the curves in the lower left plot are very steep, which indicates a very strong relationship between empty weight fraction and the required vehicle weight. Both visible curves appear to be approaching asymptotes that occur near empty weight fractions of 0.5 and 0.6 indicating that empty weight fractions less than these values are necessary for system feasibility.

The sensitivity of gross weight with energy density curves for all four different baseline cases exhibit distinctive "knees." The four curves are nearly identical for all three years, which indicates that the electrical system efficiency improvements assumed across these different years make relatively little difference when compared to changes in energy density, lift-to-drag ratio, and empty weight fraction. The four inflection points occur near energy densities of 300, 425, 500, and 700 W-hr/kg for all three technology years. At moderate to high energy densities two distinctive groups of curves are visible that correspond to the two empty weight fractions with the lower empty weight fractions requiring gross weights approximately 40% less than the higher empty weight fractions.

For the 2035 time frame, there is little dependence of required gross weight on the lift-to-drag ratio for low empty weight fractions, as shown in the plot in the first row of the second column. However, for high empty weight fractions there are noticeable inflection points in the curves occurring near lift-to-drag ratios of approximately 18 or 21 depending on the baseline energy density. This indicates that the importance of L/D is directly dependent on the empty weight fraction.

For the 2050 time frame, there is a very weak dependence of the required aircraft weight on lift-to-drag ratio for both baseline empty weight fractions and both battery energy densities. The two groupings of curves—one group near 1,800 lb gross weight and the other near 2,900 lb gross weight—are a result of the two baseline empty weight fractions, which indicates that empty weight fraction has a greater influence on the required aircraft size than L/D in the far future.

Unlike the 2015 time frame, practical aircraft can be sized with $L/D = 15$ for both the 2035 and 2050 time frames for almost all empty weight fractions shown in the last row of plots. In the 2035 time frame, noticeable inflection points occur near empty weight fractions of approximately 0.58 and 0.62 for the two different $L/D = 15$ curves. For the $L/D = 25$ curves in 2035 and all curves in 2050, there is still a noticeable decrease in required aircraft size when going from empty weight fractions of 0.7 to 0.4, however

D. Design and Technology Implications

Based on the results from all the sizing sensitivity studies, design characteristics that will most improve mission performance of fully-electric aircraft, particularly in the short term, include high lift-to-drag ratios, low empty weight fractions, and high battery energy densities. While this result is intuitive, these studies also give insight into the levels of these parameters that can provide large benefits in system performance, which can lead to the development of practical aircraft in the near future. The "knees" in the curves indicate that aircraft with cruise lift-to-drag ratios of at least 16, battery energy densities of at least 400 W-hr/kg, and empty weight fractions of less than approximately 0.5 will provide substantial mission performance increases for four-passenger aircraft compared to aircraft that do not meet these design parameters. It should be emphasized that for certain baseline values, these three levels may not be sufficient to create practical aircraft; however, these values can be viewed as thresholds above which feasibility is much more likely.

In contrast to the large benefits possible with improved L/D, battery energy density, and empty weight fraction, future technology advances in the electrical system efficiency of fully electric aircraft are considerably less important in terms of the required aircraft size. This result indicates that designers should focus less

on electrical system efficiency than achieving high L/D values, low empty weight fractions, and high energy densities.

The validity of these design and technology implications can be examined by studying existing fully electric aircraft and determining how these implications compare to those designs. Table 8 contains specifications of the first and second place aircraft in the 2011 NASA/CAFE Foundation Green Flight Challenge: the Pipistrel Taurus G4 and the University of Stuttgart e-Genius. The Taurus G4 is a four-passenger, twin fuselage aircraft that has a lift-to-drag ratio of 28 at 100 mph and can cruise for approximately 250 miles.[33] The e-Genius aircraft boasts similar range in a two-place, high wing aircraft.[34]

Table 8. Green Flight Challenge Top Aircraft Characteristics

	Pipistrel Taurus G4[33]	Univ. of Stuttgart e-Genius[34]
Gross Weight (lb)	3,307	1,874
Empty Weight (lb)	1,393	–
Empty Weight Fraction	0.4213	–
Battery Weight (lb)	1,102	–
Cruise L/D	28	–
Wing Area (ft^2)	232	153.9
Motor Power (hp)	201	80.5

The Taurus G4 has a low empty weight fraction and high L/D, which follows the design implications listed above; however, the battery energy density is approximately half of the threshold listed above. This difference in battery energy density is compensated for by the very low empty weight fraction and the very high lift-to-drag ratio of the aircraft, which is 75% higher than the value recommended above.

Each of these designs is atypical for four-place, general aviation aircraft. Tomažič et al. attribute the success of the Taurus G4 in the Green Flight Challenge to "the combination of configuration, structural efficiency, aerodynamic efficiency and the unique electric powertrain."[33] This structural efficiency is achieved through span loading of the aircraft mass laterally through the twin fuselage, which allows for a very low empty weight fraction for an aircraft with an aspect ratio of over 21. Innovative design features like this are particularly important for early electric aircraft that are likely to be mass challenged due to the poor specific energy of existing batteries.

V. Future Work

As technologies continue to improve, the practicality of fully electric aircraft will continue to increase. Research focusing on the possibilities that can be opened with this new propulsion system technology is in its infancy. In the short term, the efforts described in this paper will be expanded. In this section, an overview of the short-term future work efforts are presented.

A more detailed analysis and sizing process is possible with the use of the FLOPS software. While FLOPS was developed initially for conventionally-powered aircraft it does have the ability to analyze fully electric aircraft. Analyzing electric concepts in FLOPS would allow for more detailed mission analysis including takeoff, climb, and landing. Additionally, FLOPS would allow for evaluation of the required C rating during high power setting portions of flight to more accurately predict aircraft range.

Based on the results presented in this paper, a new concept that uses modest, evolutionary improvements will be analyzed to further investigate the feasibility of non-revolutionary airframe designs as a part of a fully electric aircraft system. This concept is inspired by a hydrogen fuel cell electric concept developed by the Naval Research Laboratory (NRL) called the Ion Dasch, which is shown in Fig. 9.[35] This concept eliminates fuselage scrubbing drag by moving the motors to the V-tail, which also improves visibility and reduces the noise and vibration caused by the motors in the passenger cabin. By mounting the motors high on the V-tail, larger propellers that can be driven at lower speeds are possible to increase propulsive efficiency without requiring long landing gear. This motor placement may also allow for the motors to be closer to the aircraft center line to reduce the motor-out yawing moment. Additionally, due to FARs, using two motors may allow the aircraft to have a stall speed greater than the 61 knots required for single-engine aircraft, as long as a

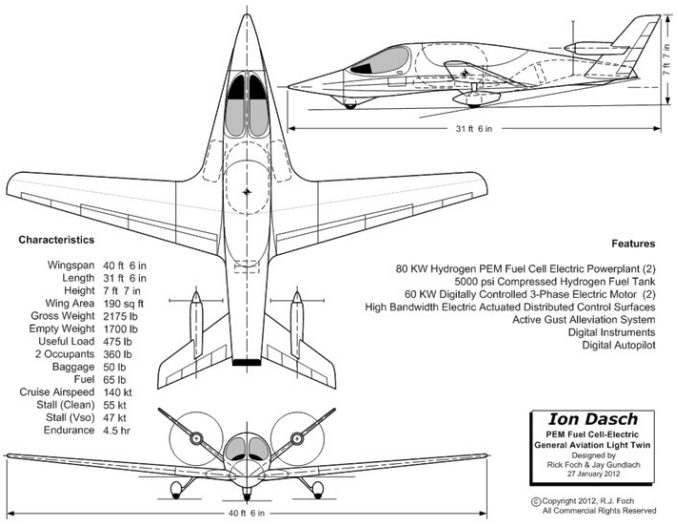

Figure 9. NRL Ion Dasch Concept[35]

minimum rate of climb is possible with one motor inoperative.[26] A higher stall speed can allow the wing to be sized more optimally for cruise conditions. Modifications to the concept will be made to account for four passengers, remove the hydrogen tank and fuel cells, and include batteries in a structurally efficient manner. The resulting configuration will be sized using the procedures presented in this paper, and the resulting performance will be analyzed.

Other new aircraft concepts may be developed that seek to capitalize on the benefits of electric propulsion through careful propulsion system integration. Design features that may be studied include those employed by the Taurus G-4 and the e-Genius as listed below.

1. Structural efficiency through span loading of payload and battery weight
2. Elimination of fuselage scrubbing drag
3. Laminar flow nose
4. Unconventional center wing section with propeller blowing to increase velocity and obtain a high $C_{L_{max}}$
5. Increased velocity on control surfaces to increase effectiveness
6. Large propeller with a large mass flow without landing gear extension

Additionally, small general aviation aircraft typically have lower wing loadings than larger aircraft due to FAR stall speed requirements.[26] Other design features that can "right-size" a wing for cruise conditions include dedicated vertical thrust-producing motors to reduce stall speed and distributed propulsion over the top surface of the wing to increase $C_{L_{max}}$ may be considered.

VI. Conclusions

The introduction of fully electric propulsion systems may fundamentally change the way small, general aviation aircraft should be operated and designed. Propulsion system characteristics such as zero thrust lapse with altitude will effect the required power, potentially changing which sizing constraints are active compared to legacy aircraft. Smaller motor sizes and weights may allow for distributed propulsion and reduced vehicle drag through careful propulsion system integration. Other aircraft system-level characteristics such as constant vehicle weight during cruise, zero emissions, low noise, and the difficulty of removing batteries can change the manner in which electric aircraft are operated. For example, cruise climbs are not required for constant weight vehicles to obtain optimum performance, and it will be difficult to trade payload weight and fuel weight for extended range as with conventionally-fueled aircraft.

While simplified Breguet-like analyses can indicate general trends for electric aircraft performance and provide estimates of necessary technology levels, more detailed analyses are required to fully study the practicality of electric aircraft propulsion. For example, Breguet range analysis is not sufficient to determine if the required discharge rate (C rating) of the batteries during takeoff or other high-power flight conditions can be practically achieved. Additional studies utilizing FLOPS or other more-detailed performance analysis tools are required to understand all practical limits of current electric propulsion system technology and the improvements that are required before electric aircraft can be practically introduced.

The results of the studies in this paper indicate that with 2015-era technologies, small, general aviation class electric aircraft that are simple modifications to existing airframes will likely not be practical for widespread operation despite the large weight saving realized by removing the engine and replacing it with a motor. For these aircraft, the weight savings that are gained by removing the engine are lost due to the heavy batteries that are required by the low energy densities of current and near-term battery technologies. Far-future technology predictions do improve the practicality of electric aircraft created from simple modifications to existing airframes; these aircraft will likely have lower range capability than conventional aircraft with low to moderate payloads, but may potentially be capable of increased ranges for higher payload weights.

In order to create practical, general aviation class, fully electric aircraft in the near term, completely new concepts designed around the electric propulsion system will be necessary. These designs will require higher than usual L/D ratios and lower empty weight fractions than are typically found in general aviation aircraft to be viable. These concepts should also consider careful, synergistic integration of the propulsion system and airframe in order to maximize performance. If designed wisely, fully electric aircraft may become a new, efficient, fast, and clean mode of transportation.

Acknowledgments

This work was performed under National Institute of Aerospace Task 6322, NASA # NNL12AB26T.

References

[1]Wells, D., "NASA Green Flight Challenge: Conceptual Design Approaches and Technologies to Enable 200 Passenger Miles per Gallon," *11th AIAA Aviation Technology, Integration, and Operations (ATIO) Conference, including the AIAA Balloon Systems Conference and 19th AIAA Lighter-Than-Air Technology Conference*, Virginia Beach, VA, Sept 20–22 2011, AIAA-2011-7021.

[2]Steitz, D. E., "NASA Awards Historic Green Aviation Prize," Press Release 11-334, NASA Headquarters, Oct 3 2011, http://www.nasa.gov/home/hqnews/2011/oct/HQ_11-334_GFC_Winners.html.

[3]Miranda, L. R. and Brennan, J. E., "Aerodynamic Effects of Wingtip-Mounted Propellers and Turbines," *Applied Aerodynamics Conference, 4th*, San Diego, CA, June 9–11 1986, pp. 221–228, AIAA-86-1802.

[4]Abeyounis, W. K., Patterson, James C., J., Stough, H. P., I., Wunschel, A. J., and Curran, P. D., "Wingtip Vortex Turbine Investigation for Vortex Energy Recovery," *SAE Aerospace Technology Conference and Exposition*, SAE Paper 901936, October 1–4 1990.

[5]Smith, J. C. and Viken, J., "Projected Demand and Potential Impacts to the National Airspace System of Autonomous, Electric, On-Demand Small Aircraft," *12th AIAA Aviation Technology, Integration, and Operations (ATIO) Conference and 14th AIAA/ISSMO Multidisciplinary Analysis and Optimization Conference*, Indianapolis, IN, Sept 17–19 2012, AIAA-2012-5595.

[6]Moore, M. D., "Concept of Operations for Highly Autonomous Electric Zip Aviation," *12th AIAA Aviation Technology, Integration, and Operations (ATIO) Conference and 14th AIAA/ISSMO Multidisciplinary Analysis and Optimization Conference*, Indianapolis, IN, Sept 17–19 2012, AIAA-2012-5472.

[7]Fredericks, W. J. and Moore, M. D., "Benefits of Hybrid-Electric Propulsion to Achieve 4x Cruise Efficiency for a VTOL UAV," *12th AIAA Aviation Technology, Integration, and Operations (ATIO) Conference and 14th AIAA/ISSMO Multidisciplinary Analysis and Optimization Conference*, Indianapolis, IN, Sept 17–19 2012, AIAA-2012-5473.

[8]Moore, M. D., "Design Study of a Hybrid-Electric Aircraft for On-Demand Aviation," *12th AIAA Aviation Technology, Integration, and Operations (ATIO) Conference and 14th AIAA/ISSMO Multidisciplinary Analysis and Optimization Conference*, Indianapolis, IN, Sept 17–19 2012, AIAA-2012-5515.

[9]McCullers, L. A., "Aircraft Configuration Optimization Including Optimized Flight Profiles," *NASA Langley Research Center Recent Experiences in Multidisciplinary Analysis and Optimization, Part 1*, 1984, pp. 395–412.

[10]McCullers, L. A., *FLOPS Users Guide, Release 6.02*, NASA Langley Research Center, March 2003.

[11]Imagine Air Jet Services, LLC, http://www.flyimagineair.com/, accessed 20 Aug 2012.

[12]Skyway Air Taxi, http://www.skywayairtaxi.com/, accessed 20 Aug 2012.

[13]OpenAir, http://www.flyopenair.com/, accessed 20 Aug 2012.

[14]"Pilot's Operating Handbook and EASA Approved Airplane Flight Manual for the Cirrus Design SR22," Revision A9 13772-001E, Cirrus Design Corporation, 4515 Taylor Circle, Duluth, MN 55811, Oct 2003.

[15]Hahn, A. S., "Vehicle Sketch Pad: A Parametric Geometry Modeler for Conceptual Aircraft Design," *48th AIAA Aerospace Sciences Meeting Including the New Horizons Forum and Aerospace Exposition*, Orlando, Florida, January 4–7 2010, AIAA-2010-657.

[16]OpenVSP, http://www.openvsp.org/, accessed 28 Aug 2012.

[17]Cirrus Design Corporation, "SR22 Specifications: Payload Chart," http://cirrusaircraft.com/sr22/, 2011, accessed 22 July 2012.

[18]Deperrois, A., "XFLR5," 2012, http://www.xflr5.com/xflr5.htm.

[19]Raymer, D. P., *Aircraft Design: A Conceptual Approach*, American Institute of Aeronautics and Astronautics, 4th ed., 2006.

[20]Feagin, R. C. and Morrison, William D., J., "Delta Method, An Empirical Drag Buildup Technique," NASA Contractor Report 151971, NASA, December 1978.

[21]Corsiglia, V. R., Katz, J., and Kroeger, R. A., "Full-Scale Wind-Tunnel Study of the Effect of Nacelle Shape on Cooling Drag," *Journal of Aircraft*, Vol. 18, No. 2, February 1981, pp. 82–88.

[22]Katz, J., Corsiglia, V. R., and Barlow, P. R., "Cooling Air Inlet and Exit Geometries on Aircraft Engine Installations," *Journal of Aircraft*, Vol. 19, No. 7, July 1982, pp. 525–530.

[23]Mattingly, J. D., *Elements of Propulsion: Gas Turbines and Rockets*, American Institute of Aeronautics and Astronautics, Inc., 1801 Alexander Bell Drive, Reston, Virginia 20191, 2006.

[24]Willford, N., "Cool It! Engine cooling and drag reduction," *EAA Sport Aviation Magazine*, August 2003, pp. 50–56.

[25]Geiselhart, K., "ENGGEN Engine Cycle Analysis Program Release 4.0 User's Guide," Tech. rep., NASA Langley Research Center, 2009.

[26]"Stalling speed," *Code of Federal Regulations*, Title 14, Part 23.49, 2012.

[27]Nam, T., *A Generalized Sizing Method for Revolutionary Concepts under Probabilistic Design Constraints*, Ph.D. thesis, Georgia Institute of Technology, April 2007.

[28]"Fuel requirements for flight in VFR conditions," *Code of Federal Regulations*, Title 14, Part 91.151, 2012.

[29]"Fuel requirements for flight in IFR conditions," *Code of Federal Regulations*, Title 14, Part 91.167, 2012.

[30]Gallagher, K., "Envia Systems Achieves World Record Energy Density for Rechargeable Lithium-Ion Batteries," Press release, Gallagher Group Communications, Newark, CA, Feb 27 2012, http://enviasystems.com/pdf/Press_Release_400WHK.pdf.

[31]Continental Motors, Inc., *IO-550 Permold Series Engine Installation & Operation Manual*, Aug 2011, Publication OI-16.

[32]"Airplane categories," *Code of Federal Regulations*, Title 14, Part 23.3, 2012.

[33]Tomažič, T., Plevnik, V., Veble, G., Tomažič, J., Popit, F., Kolar, S., Kielj, R., Langelaan, J. W., and Miles, K., "Pipistrel Taurus G4: on Creation and Evolution of the Winning Aeroplane of the NASA Green Flight Challenge 2011," *Strojniški vestnik - Journal of Mechanical Engineering*, Vol. 57, No. 12, 2011, pp. 869–878.

[34]Institut fr Flugzeugbau, "e-Genius," http://www.ifb.uni-stuttgart.de/index.php/forschung/flugzeugentwurf/hydrogenius/318, accessed 28 Aug 2012.

[35]Foch, R. J. and Gundlach, J., "Ion Dasch PEM Fuel Cell-Electric General Aviation Light Twin," 27 Jan 2012.